Journal of Alloys and Compounds 773 (2019) 940–949

Contents lists available at ScienceDirect

Journal of Alloys and Compounds

journal homepage: http://www.elsevier.com/locate/jalcom

Effect of oligocrystallinity on damping and pseudoelasticity of oligocrystalline Cu-Al-Mn shape memory foams

Hua Li [a], Bin Yuan [a, b], Yan Gao [a, b, *], Yuyuan Zhao [c]

[a] School of Materials Science and Engineering, South China University of Technology, Guangzhou, 510640, PR China
[b] Key Laboratory of Advanced Energy Storage Materials of Guangdong Province, PR China
[c] School of Engineering, Universtiy of Liverpool, Liverpool, L69 3GH, United Kingdom

ARTICLE INFO

Article history:
Received 6 August 2018
Received in revised form
14 September 2018
Accepted 17 September 2018
Available online 18 September 2018

Keywords:
Cu-based shape memory alloy
Metal foams
Cyclic heat treatment
Grain growth
Grain constraints

ABSTRACT

Oligocrystalline Cu-Al-Mn shape memory foams with a pore size of 0.8–1.1 mm and a porosity of ~70% were prepared by the silica-gel beads infiltration method, subjected to long-time and cyclic heat treatments. The effect of grain size and oligocrystallinity (ratio of grain size to strut node diameter) on the damping and pseudoelastic properties of the foams were investigated. The peak damping increases with oligocrystallinity because a higher oligocrystallinity favors the martensite accommodation and mobility of phase interfaces during martensitic transformation. The low-amplitude martensite damping first increases and then decreases with increasing oligocrystallinity, because the martensite plates grow wider in larger grains with lower grain constraints, leading to fewer interfaces and lower damping. The high-amplitude martensite damping increases linearly with increasing oligocrystallinity, despite the wider martensite plates and reduced interfaces, indicating that the mobility of martensite plates for higher displacements is more favored by reduced grain constraints. The maximum recovery strain increases linearly with oligocrystallinity and a high value of 5.53% was achieved after cyclic heat treatment for 16 times, corresponding to an oligocrystallinity of 7.88. The high recovery strain results from the reduced triple junctions and grain boundary area due to grain enlargement that lowers the grain constraints.

1. Introduction

Shape memory foams (SMF), or porous shape memory alloys (SMA), have attracted many interests due to their multi-functional properties arising from the combination of the porous structure and a shape memory alloy matrix [1–3]. More recently, oligocrystalline shape memory foams (oSMF) become an active research area because of the greatly improved damping and pseudoelastic properties derived from the additional benefits of the oligocrystalline microstructure [4,5]. Cu-based SMFs and oSMFs are particularly promising for applications in civil engineering and automotive industry for their low cost, good workability and relatively high functional properties [6].

Dense Cu-based oligocrystalline shape memory alloys (oSMA) have been well studied in recent years [7–10]. Oligocrystalline microstructure, which is defined as one where the total surface area exceeds the total grain boundary area and triple junctions are almost absent [7], can exist in fine wires [8], thin sheets [9] and rods [10]. These Cu-based oSMAs are free of three-dimensional grain constraints and severe stress concentration at triple junctions, leading to their greatly improved damping and pseudoelastic properties. However, research on the processing, characterization, and properties of open-cell oSMFs is still very limited [4,5], due to the complex strut architecture in the SMFs. Oligocrystalline Cu-based SMFs with an irregular foam structure, fabricated by directional solidification, showed improved properties due to enlarged grains [4]. Quantitative analysis of Cu-based oSMFs with spherical pore morphology has been carried out [5].

The three-dimensionally linked strut architecture of open-cell foams makes it possible to form oligocrystalline microstructure when the grain size becomes large enough to span the full cross-section of the struts. The effect of strut sizes on the formation of oligocrystalline microstructure, however, is twofold [5]. On the one hand, thinner struts tend to allow more grains to span the strut cross sections and therefore increase the oligocrystallinity. On the other

* Corresponding author. School of Materials Science and Engineering, South China University of Technology, Guangzhou, 510640, PR China.
E-mail address: meygao@scut.edu.cn (Y. Gao).

https://doi.org/10.1016/j.jallcom.2018.09.206
0925-8388/

hand, too thin and short struts may constrict grain growth [5,11] and become an unfavorable factor for oligocrystalline microstructure formation. The foam structure not only influences the formation of the oligocrystalline microstructure but also affects the basic mechanical and functional properties of SMFs [5,12–14]. Imperfections and irregular pore size should be avoided since they may cause high stress-concentration [15] and undesirable effect on the properties [16]. Therefore, the foam structure needs to be well controlled and well defined to fully exploit the benefits of the oligocrystalline microstructure without the adverse effect of the foam structure.

In an oSMF with a fixed pore structure, grain size becomes the only factor determining the oligocrystallinity. To form an oligocrystalline microstructure, the grains should be large enough to span the strut cross-sections. Larger grains are preferred in order to eliminate or reduce the triple junctions where stress concentration is severe [17]. Large grains can also reduce the total area of grain boundaries and therefore reduce grain constraints around the grain boundaries, which may cause partial transformation [17]. In other words, large grains are preferable because they reduce the probability of fracture near triple junctions and expand the unconstrained regions where the deformation can be accommodated more freely [17], thus improving the performance of the oSMFs.

Cu-Al-Mn SMFs with uniform and spherical pore morphology, the porosity of ~70%, the pore size of 0.8–1.1 mm, and millimeter-sized coarse grains have been obtained by the silica-gel beads molten metal infiltration method [5]. The intrinsic coarse grain feature of the Cu-based SMAs, which is the main factor causing the brittleness in traditional polycrystalline Cu-based SMAs [18], becomes an advantage for preparing oSMFs. However, triple junctions still existed in the resultant SMFs because of the complex three-dimensional strut architecture of the foam materials [5,19]. Further grain enlargement is still required in order to eliminate the triple junctions and expand the unconstrained area.

There is a limited number of methods to enlarge the grains of SMFs. The conventional strain-annealing method is not suitable for metal foams because it calls for macroscopic deformation to provide the driving force for grain growth in the subsequent annealing procedure [20]. Heat treatment becomes the only practical approach for grain enlargement in foams. A cyclic heat treatment (CHT) method has been reported to successfully trigger abnormal grain growth without introducing macroscopic deformation in dense Cu-Al-Mn SMAs with a high content of Mn [21]. These Cu-Al-Mn samples were cyclically heated and cooled between the high-temperature single β region and the low temperature two-phase α+ β region. A sub-grain microstructure was reported to have occurred during the precipitation and dissolution of the α phase, which may have provided the driving force for the grain growth [21].

In this paper, both the traditional long-time heat treatment (LHT) at a constant elevated temperature and the cyclic heat treatment (CHT) methods were carried out on a series of Cu-Al-Mn foam samples with almost identical pore structures, produced by the silica-gel bead infiltration method. The effects of the heat treatment procedures on grain growth were investigated. The effect of grain size and accordingly the oligocrystallinity on the damping and pseudoelastic behavior of the Cu-Al-Mn SMF was investigated. The aim of the work is to provide some guidance for the development and optimization of Cu-based oSMF in general and Cu-Al-Mn oSMF in particular since Cu-Al-Mn SMA is more promising among the Cu-based SMAs due to its good ductility [22].

2. Experimental

2.1. Materials and heat treatments

Several Cu-18.5Al-11Mn (at.%) SMF samples with a pore size of 0.8–1.1 mm and a porosity of ~70% were prepared by the silica-gel beads infiltration method, the details of which have been reported in our previous work [5]. The foaming process was conducted in a vertical tube furnace equipped with a vacuum and argon gas system. The Cu-18.5Al-11Mn mother alloy block prepared by an induction melting method was melted at 1100 °C for 15 min in a high vacuum of 10^{-3} Pa and was then infiltrated into the underneath silica-gel beads bed by introducing an argon gas with a pressure of 0.18 MPa. The pore morphology and structure can be controlled by adjusting the expansion and mutual squeezing degree of the spherical silica-gel beads which can be completely dissolved by the 25% HF aqueous solution. The silica-gel beads density for preparing these foams was about 0.80–0.85 g cm^{-3}.

The macro and SEM images of a Cu-Al-Mn foam sample are shown in Fig. 1 (a) and (b), respectively. The sample exhibits a uniform open cell morphology with spherical pores interconnected three-dimensionally with each other. The metal matrix is a three-dimensional network of thin struts, connected with each other via strut nodes, between the pores.

Two heat treatments, long-time heat treatment (LHT) and cyclic heat treatment (CHT), were used, as shown schematically in Fig. 2 (a) and (b), respectively. The heat treatments were conducted in a box-type electrical resistance furnace. The foam samples were sealed in quartz tubes filled with argon of one atmospheric pressure to reduce oxidization and volatilization of the alloying elements. In order to enlarge the grains as much as possible and to avoid overheating at the same time, a relatively high temperature of 930 °C was chosen as the heating temperature, which is about 50 °C below the melting point of the Cu-18.5Al-11Mn alloy. For the long-time heat treatment, five Cu-18.5Al-11Mn SMF samples were heated at 930 °C for 20 min, 3, 9, 12 and 24 h, respectively, and then quenched into water with the quartz tubes being broken simultaneously. For the cyclic heat treatment, four Cu-18.5Al-11Mn SMF samples were heated at 930 °C for 30 min, cooled to 500 °C for 15 min and then heated back to 930 °C, with the cooling and heating rates being 3 °C/min and 10 °C/min, respectively. This cycle was repeated for 2, 10, 16 and 20 times, with the total holding time at 930 °C of 1.5, 5.5, 8.5 and 10.5 h respectively, followed by water quenching from 930 °C. After water quenching, all the samples were immediately subjected to a low-temperature aging at 150 °C for 20 min to stabilize the transformation temperatures [23].

2.2. Measurement of oligocrystallinity

The spatial architecture of foam materials is made up of metal struts interconnected three-dimensionally at strut nodes, as shown in Fig. 1 (b). The oligocrystallinity, or oligocrystalline degree, of oSMFs can be characterized by the ratio of grain size d to the strut node size N (d/N) [5], in analogy with the ratio of grain size to wire diameter (d/D) [24] or to sheet thickness (d/t) [9] for dense oSMAs. Since the strut nodes are the widest place of the struts, higher oligocrystallinity (d/N) means that it is easier for the grains to cover the whole cross-section of the struts and thus leads to less triple junctions in oSMFs. The oligocrystallinity (d/N) also represents the ratio of free surface area to the grain boundary area of the oSMFs. Higher oligocrystallinity (d/N) corresponds to a larger unconstrained area near the free surface than the constrained area near grain boundary and triple junctions.

The oligocrystallinity (d/N) of the SMF samples subjected to different heat treatments was determined by measuring the average two-dimensional grain size, d_{2D}, and the average two-dimensional diameter of the strut nodes, N_{2D}, as illustrated in Fig. 3 d_{2D} and N_{2D} are the cross-sectional intercepts of d and N of the three-dimensional structure, respectively. According to quantitative stereology [25], the average grain size and strut node size can

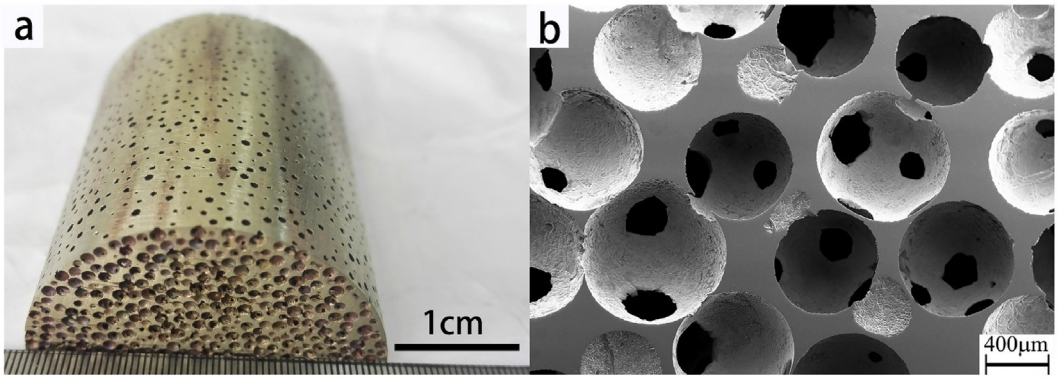

Fig. 1. (a) Macro and (b) SEM images of the Cu-Al-Mn foams with a pore size of 0.8–1.1 mm and a porosity of about 70% prepared by the silica-gel beads infiltration method.

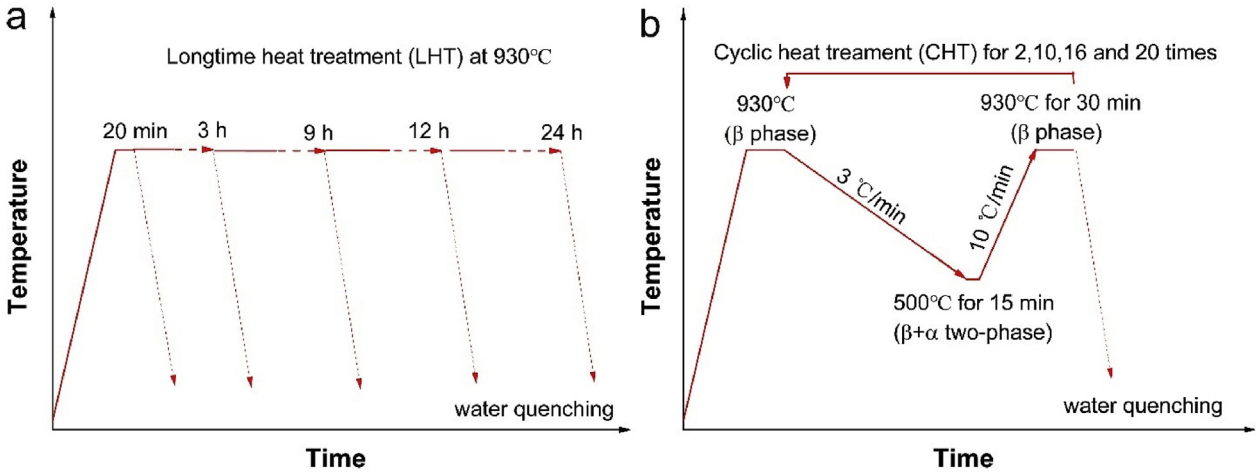

Fig. 2. Schematic procedures of (a) long-time heat treatment and (b) cyclic heat treatment processes.

be calculated by $d=\frac{4}{\pi}d_{2D}$ and $N=\frac{4}{\pi}N_{2D}$, respectively, if the strut nodes and grains are simply assumed to be spheres.

The average two-dimensional node size, N_{2D}, of the foam samples with a porosity of ~70% and pore size of 0.8–1.1 mm was calculated by the Image-Pro Plus 6.0 software using at least five optical images with 100–150 counts in total and was determined to be about 0.41 mm [5]. The average two-dimensional grain size, d_{2D}, was measured on the optical images of the foam samples, which

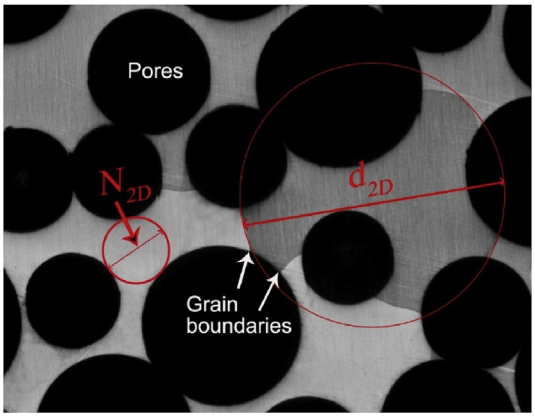

Fig. 3. Schematic diagram for strut node size (N) and grain size (d) measurements on an OM image.

was carefully polished and etched by the HCl-$FeCl_3$ solution. Because the grains may grow too large to be measured accurately on a single image, a large image spliced by several optical images, with 50–80 grains in total was used for the measurement. Only the grains fully contained within the spliced image were considered.

2.3. Characterization of damping and pseudoelastic properties

The damping property of the foam samples was characterized by measuring the internal friction, tanδ by a TA-Q800 Dynamic Mechanical Analyzer (DMA) in the single cantilever mode with a gauge length of 17.5 mm. The foam specimens with dimensions of 30 mm × 8 mm × 1.5 mm were prepared by wire-electrode cutting. The low-amplitude internal friction was tested with a frequency of 1 Hz and a strain amplitude of 0.05% while cooling the samples from 150 °C to −120 °C at a rate of 5 °C/min. The tanδ-(strain-amplitude) curves in the martensite state were tested isothermally at a temperature 50 °C below the martensite finish temperature (M'_f −50 °C) with a constant frequency of 1 Hz and strain amplitude sweeping from ~0.02% to ~2.00%.

The pseudoelastic property of the foam samples was tested by an Instron 5984 testing system equipped with an insulation chamber. The foam specimens were cut into dimensions of about Φ10 mm × 15 mm with both bearing surfaces carefully polished and coated with lubricating oil to reduce friction. The specimens were heated in the chamber to a temperature 30 °C above the austenite finish temperature (A_f +30 °C), which is about 55 °C for

our materials, and maintained for 20 min before testing. The cyclic compression test was carried out isothermally by cyclically loading and unloading at a rate of 0.1 mm/min, while gradually increasing the applied strain of each cycle from 1% to 8%.

3. Results and discussion

3.1. Grain size and oligocrystallinity

Fig. 4 shows the optical micrographs of the Cu-Al-Mn SMFs after long-time and cyclic heat treatments, where the grain boundaries are marked by white arrows. It is seen that the grains expand across the whole cross-sections of the struts with the grain boundaries perpendicular to the pore surface and no triple junctions are observed in these foam samples, showing an oligocrystalline microstructure.

The average grain size *d* and oligocrystallinity *d/N* of all specimens are listed in Table 1. Their relationship with the holding time at 930 °C for LHT and CHT is shown in Fig. 5(a). Similar trends are observed in both curves, with *d* and *d/N* increasing sharply at the beginning and then leveling off towards an asymptotic line. The average grain size of the sample after LHT for 9 h is about 2.93 mm, with the corresponding *d/N* of about 6.98. By comparison, the average grain size of the sample after CHT for 20 cycles (10.5 h) is 3.44 mm, with the corresponding *d/N* of about 8.19. It is clear that the grain growth after cyclic heat treatment is much greater than that after long-time heat treatment.

Although the grain growth of our Cu-Al-Mn foam samples after CHT is impressive, it is far from satisfactory when compared with Cu-Al-Mn sheets after CHT, where the grains grow to 10–20 mm after the first cycle and over 35 mm after the fifth cycle [21]. Even the largest grains observed in our Cu-Al-Mn foams subjected to CHT are only about 8–10 mm after cycling for 10–20 times, as shown in Fig. 4(e–g). The microstructural principle that encourages grain growth in Cu-Al-Mn sheets by CHT should also work in our Cu-Al-Mn foams. Fig. 5(b) shows the microstructure of the Cu-Al-Mn SMF sample at the lower temperature of the CHT procedure, obtained by water quenching from 500 °C after cooling from 930 °C and annealing for 15 min. This is a two-phase microstructure with α phase embedded in β phase grains, which is the microstructural foundation to realize the abnormal grain growth by cyclic heat treatment. Sub-grains of 25–50 μm were observed in the SMF samples after CHT for 16 cycles (Figs. 3(f) and 7(e)). These sub-grains, formed during cyclic precipitation and dissolution of the α phase, may provide the main driving force for the abnormal grain growth [21].

Some other reasons may be responsible for the different grain growth between foams and sheets. First, the sheets were rolled before the cyclic heat treatment [21]. As a consequence, the energy stored in the defects and grain boundaries may provide an extra driving force for grain growth during heat treatment. Second, the sheets have a much larger size in the in-plane dimension than the length of the foam struts, making grain growth in sheets free from the restriction effect in length dimension. It is reported that the grain size of Cu-Al-Mn oSMFs increases linearly with strut length [5], whereas the sheets can be regarded as the foam struts with an infinite length. Third, the sheets have less surface area than the foams. It is reported that the grain growth in oligocrystalline sheets can be hindered by surfaces because surface energy becomes significant and grain boundaries tend to be dragged by grooves and steps formed on surfaces [11]. This is more pronounced for grain growth in oSMFs because of the larger specific surface area that leads to a decrement in the ratio of grain size to strut length [5]. Unlike in sheets with two parallel surfaces, the grains in foams grow across the strut nodes and come across several other adjacent strut branches sharing the same node. It is more difficult for the grains to grow because they have to overcome a much higher surface area in total that hinders grain boundary migration.

3.2. Dependence of damping on heat treatment and oligocrystallinity

3.2.1. tanδ-temperature curves and limit of heat treatment time

Fig. 6(a) and Fig. 6(b) show the tanδ-temperature curves of the Cu-Al-Mn SMFs subjected to long-time and cyclic heat treatments, respectively, obtained by the DMA with a strain amplitude of 0.05%, frequency of 1 Hz and cooling rate of 5 °C/min. The internal friction spectrums of the SMFs are clearly divided into three regions: the low-temperature region in martensite state with a relatively high damping plateau, the intermediate-temperature region in the transformation region with the damping peak, and the high-temperature region in austenite state with a relatively low

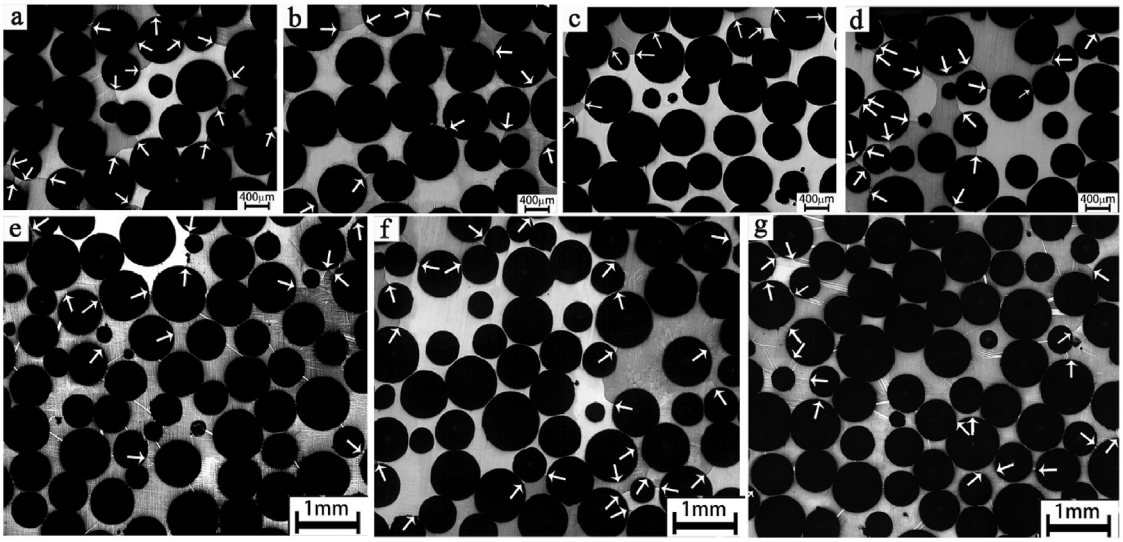

Fig. 4. Optical micrographs of the Cu-Al-Mn SMFs subjected to long-time heat treatments at 930 °C for (a) 20 min, (b) 3 h and (c) 9 h and cyclic heat treatment between 930 °C and 500 °C for (d) 2 times, (e) 10 times, (f) 16 times and (g) 20 times. The grain boundaries are marked by white arrows.

Table 1
The average grain size (d), oligocrystallinity (d/N), internal friction (tanδ) and maximum recovery strain (ε_R^{MAX}) values for the Cu-Al-Mn SMFs subjected to different heat treatments.

Samples	Total holding time at 930 °C [hours]	d [mm]	d/N	M damping (0.05% strain)	Peak damping	M damping (1.90% strain)	ε_R^{MAX}[%]
930 °C × 20 min	0.33	1.67	3.98	0.0468	0.093	0.213	4.15
CHT × 2	1.5	2.10	5.00	0.0579	0.108	0.224	4.45
LHT × 3 h	3.0	2.67	6.36	0.0627	0.118	0.245	4.93
LHT × 9 h	9.0	2.93	6.98	0.0570	0.132	0.253	5.11
CHT × 10	5.5	3.06	7.29	0.0510	0.141	0.257	5.30
CHT × 16	8.5	3.31	7.88	0.0488	0.152	0.260	5.53
CHT × 20	10.5	3.44	8.19	0.0469	0.154	0.255	/
LHT × 12 h	12.0	/	/	0.0447	0.095	0.221	/
LHT × 24 h	24.0	/	/	0.0367	0.067	0.211	/

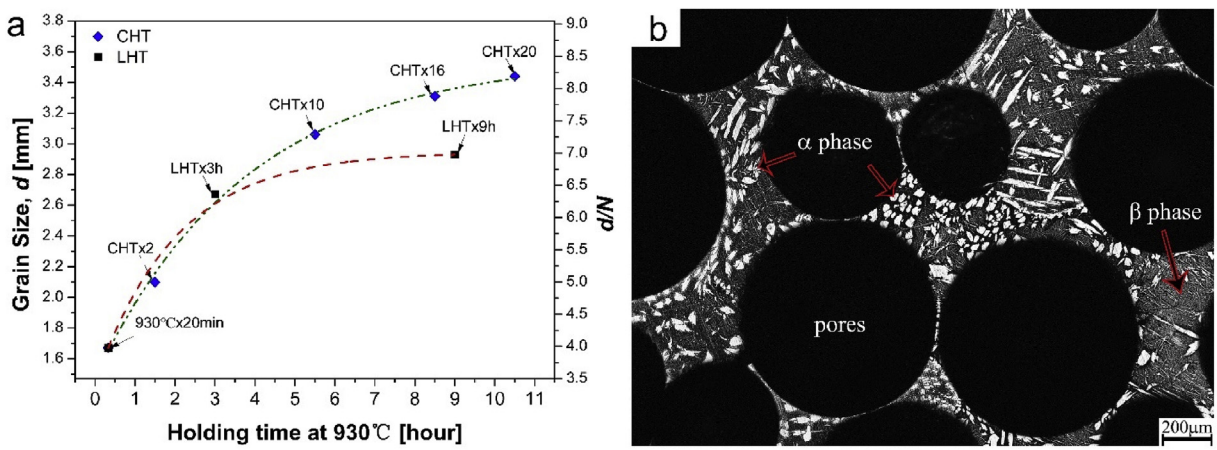

Fig. 5. (a) Relationships of average grain size d and d/N with the holding time at 930 °C for long-time and cyclic heat treatments; (b) the two-phase (β+α) microstructure of the Cu-Al-Mn foam subjected to water quenching from 500 °C after cooling from 930 °C and annealing at 500 °C for 15 min.

damping plateau. Only the martensite and transformation regions are considered in this paper. The internal friction in martensite state is represented by the tanδ value at the temperature (M_f'-50 °C), which is illustrated and marked in Fig. 6(a) for one of the curves. The tanδ values of all samples in martensite state and at peaks are listed in Table 1 and designated as M damping and peak damping, respectively.

Fig. 6(b) shows that the peak damping of the Cu-Al-Mn SMFs increases steadily with increasing number of CHT cycles all the way to 20 times (10.5 h). For the long-time heat treatment, the peak damping also increases continuously with heating time up to 9 h (Fig. 6(a)). The increase in peak damping should be attributed to the grain growth that results in lower grain constraints to favor the martensite transformation and interface movement.

When the heating time is increased to 12 h and 24 h in LHT, however, the internal friction at peaks decreases sharply to low values of 0.095 and 0.067, respectively (Fig. 6(a)). Similar deterioration is observed in the damping in the martensite state. It can also be observed that the martensite finish temperature (M'_f) and the temperature corresponding to the damping peak increase when the heating time is increased to 12 h and 24 h. The undesirable phenomena suggest that there is a limit to the heat treatment time. It seems that the maximum holding time at the high temperature of 930 °C without causing an adverse effect on damping is approximately 9–12 h.

The deterioration of damping with overlong heating time is likely a result of compositional changes in the Cu-Al-Mn foams. The Energy Dispersive Spectrum (EDS) results of the SMFs subjected to LHT with different heating time are shown in Fig. 6(c). It is seen that the contents of both Al and Mn remain reasonably constant up to 9 h but show a discernible drop as the heating time is increased to 12 and 24 h. This is consistent with the increased martensite transformation finish temperature and the damping peak temperature, which reflect their lower Al and/or Mn contents [26]. It is reasonable to deduce that the loss of Al and Mn at an overlong heating time is responsible for the damping deterioration, although the possibility of local interface melting worsening the properties cannot be excluded.

It is noticed that the martensite transformation finish temperature of the sample subjected to CHT for 20 cycles, i.e., heating at 930 °C in total of 10.5 h, shifts slightly to a higher temperature (Fig. 6(b)). Therefore, the holding time at 930 °C should not exceed 10.5 h in order to avoid overheating and undesired damping deterioration of the Cu-Al-Mn SMFs. If the samples were heated in a more aggressive environment without argon gas protection, the threshold time may be much shorter.

3.2.2. Low-strain-amplitude damping

Fig. 6(d) shows the dependence of the martensite and peak damping on oligocrystallinity, d/N. The internal friction values of the samples after LHT for 12 and 24 h, which suffered from a serious overheating problem, are excluded. It is seen that the peak damping increases monotonically with d/N, demonstrating the favorable effect of higher oligocrystallinity and lower grain constraints. The internal friction at peaks of the Cu-Al-Mn SMF subjected to CHT for 20 cycles (10.5 h) is increased by approximately 65% compared with the initial state of LHT for 20 min. The trend of the martensite damping with d/N, however, differs considerably from that of the peak damping. The tanδ–d/N curve of the martensite damping can be divided into two regions, I and II. In region I, tanδ increases to a

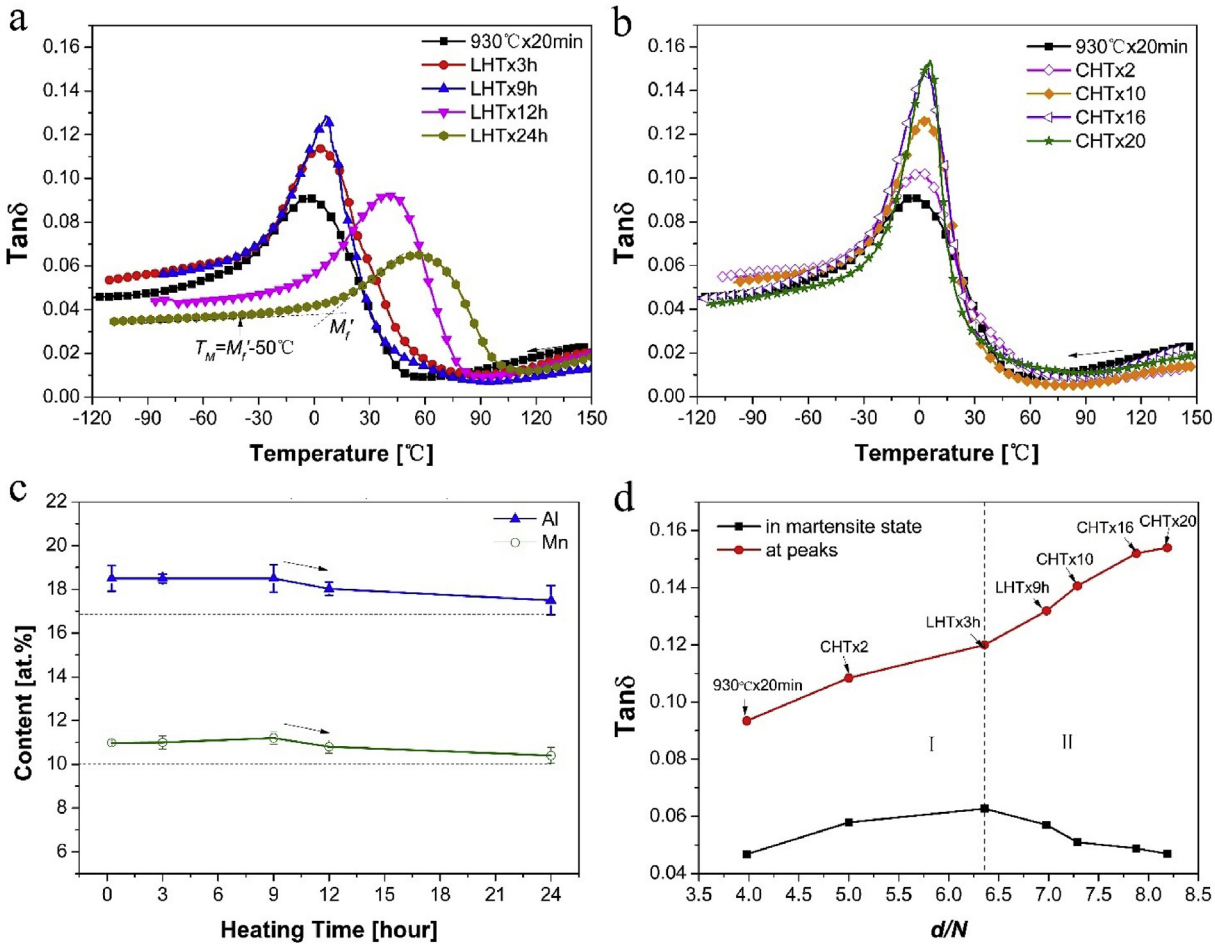

Fig. 6. Internal friction (tanδ) - temperature curves of the Cu-Al-Mn SMFs subjected to (a) long-time and (b) cyclic heat treatments; (c) Al and Mn contents as a function of heating time after LHT; (d) Dependence of the low-amplitude martensite damping and peak damping on oligocrystallinity.

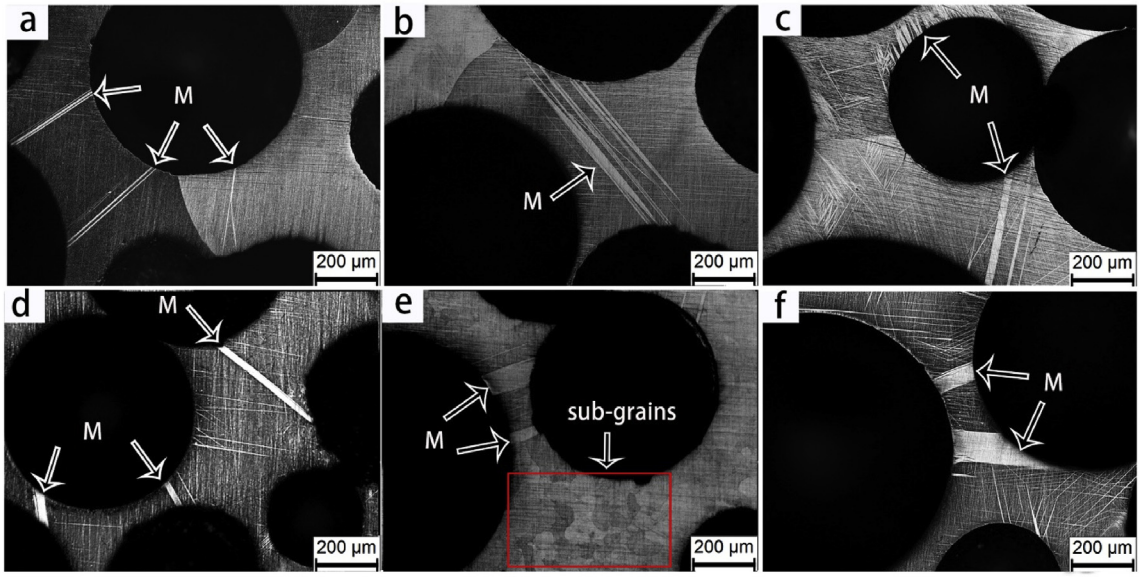

Fig. 7. Martensite microstructure of the Cu-Al-Mn SMFs after different heat treatments and with various *d*/*N* values: (a) 930 °C × 20 min (*d*/*N* = 3.98), (b) LHT × 3h (*d*/*N* = 6.36), (c) LHT × 9h (*d*/*N* = 6.98), (d) CHT × 10 (*d*/*N* = 7.29), (e) CHT × 16 (*d*/*N* = 7.88), (f) CHT × 20 (*d*/*N* = 8.19). The martensite plates are marked by arrows and the sub-grains after CHT are highlighted by the rectangular frame.

maximum of 0.627 as *d/N* increases to 6.36; In region II, tanδ decreases when *d/N* increases further from 6.36.

The different dependences of peak and martensite damping on oligocrystallinity can be attributed to the mechanism difference between damping during the martensitic transformation process and damping in pure martensite state. It is well known that the internal friction of shape memory alloys is made up of three parts [27]: transient, intrinsic and phase transition. The transient part is related to the transformation kinetics and is strongly dependent on the testing parameters. This term is the same for all the SMF samples since they were measured in the same test conditions. The intrinsic part is contributed by the austenite and martensite phases and depends on the microstructure of each phase. The phase transition term is associated with martensitic transformation and relates to the mobility of parent/martensite habit planes. As a porous material, the macropores also contribute to the damping via strut bending, cell wall reflection and movement of defects near the cell walls [28]. The damping related to the porous structure will not be considered here since it is the same for all the samples. The different behaviors in martensite and peak damping can be analyzed in terms of the roles played by the intrinsic and phase transition terms.

The damping in pure martensite state is mainly from the contributions of the intrinsic term, which relates to the microstructure and mobility of the martensite phase. The mobility of the martensite boundaries should increase with oligocrystallinity since higher *d/N* corresponds to higher unconstrained area and lower grain constraints for the martensite boundaries to move. The microstructure, and its effect on the damping, however, is different from region I to region II. Fig. 7 shows the microstructure of martensite plates of the SMFs after different heat treatments and with various *d/N* values. It can be observed that the width of the martensite plates hardly changes as *d/N* is lower than 6.36 but increases markedly with increasing *d/N* further, reaching about 100 μm as *d/N* increases to 8.19 (CHT × 20). Wider plates mean less martensite interface area, leading to reduced martensite damping in region II. Combining both microstructure and mobility effects, the overall trend is that martensite damping first increases in region I and then decreases in region II, with *d/N*. This phenomenon indicates that the microstructural change of the martensite plates is the dominant factor in low-amplitude martensite damping. The widening martensite plates also demonstrate that the oSMFs have low grain constraints. If the grain constraints were high, it was reported that it is easier for new plates to nucleate than for the existed ones to grow, which would have led to groups of thin plates rather than wider ones [17].

In peak damping which emerges during the martensitic transformation region, the intrinsic term due to the microstructure and mobility of martensite and austenite remains the same as or is less than that in pure martensite state. The phase transition term may, therefore, play a more significant role, indicating that a higher oligocrystallinity can facilitate the martensitic transformation process. Grain constraints for martensite accommodation and phase interface movements are reduced with higher *d/N,* which corresponds to less grain boundary area and fewer triple junctions. As a result, the martensite transformation can progress more smoothly and the parent/martensite habit planes can move more easily in a larger region of the unconstrained area, increasing the phase transition term of the peak damping. This enhancement in the phase transition term may be able to offset the negative effect of lower interface density on the intrinsic term, leading to a continuous increment of peak damping with increasing *d/N*.

3.2.3. High-strain-amplitude martensite damping

Fig. 8(a) and (b) show the tanδ–(strain amplitude) curves of the Cu-Al-Mn SMFs after long-time and cyclic heat treatments, respectively, obtained in the pure martensite state at a temperature of *Mf*'-50 °C. The martensite damping of all these SMF samples shows a similar trend of variation with strain amplitude. As the strain amplitude is increased, the martensite damping increases rapidly in the beginning when more martensite boundaries are involved in the longer-distance movement, then increases slowly after a threshold when no new boundaries are available, and finally approaches an asymptotic line when the movements of martensite boundaries are saturated. The martensite damping at high amplitude is seen to increase with heating time up to 9 h. Longer heating time posed an overheating problem.

The relationship of the high-amplitude martensite damping, at a strain-amplitude of 1.90%, with oligocrystallinity (*d/N*) is shown in Fig. 8(c). It is shown that the martensite damping at high strain-amplitude depends strongly on oligocrystallinity, with the internal friction increasing almost linearly with *d/N* with a linear fitting R-square of 0.983. The internal friction (tanδ) at high strain amplitude of the Cu-Al-Mn SMF sample after CHT for 16 cycles (8.5 h, $d/N = 7.88$) reaches 0.260, an enhancement of 22% over the initial state of 0.213. This enhancement is achieved despite the wider martensite plates in samples with larger grains.

The different trends of martensite damping with *d/N* at low and high strain amplitudes indicate that the martensite damping is more sensitive to the mobility of martensite plates at a high strain amplitude. At a high strain amplitude, longer-distance movements of more martensite boundaries are triggered by a larger displacement. The mobility of martensite boundaries then becomes more important to the intrinsic martensite damping. This is because a higher *d/N*, which corresponds to relaxation of grain constraints, can result in smoother longer-distance movements of martensite boundaries, leading to linearly improving high-amplitude martensite damping with *d/N*. It seems that the mobility of the boundaries is of greater influence than the interface density at high strain amplitudes, while the reverse is true at low strain amplitudes.

3.3. Dependence of mechanical and pseudoelastic properties on oligocrystallinity

Fig. 9(a–f) show the stress-strain curves of the Cu-Al-Mn SMF specimens after different heat treatments with various oligocrystallinity values, obtained by cyclic compression at a temperature 30 °C above the austenite finish temperature (A_f +30 °C). The foam specimens were cyclically loaded and unloaded. In each cycle, the specimen was compressed to a strain of ε_a^i and then unloaded, resulting in a residual strain ε_r^i, where *i* designates the ordinal number of the cycle. Eight cycles were performed and the applied strain, ε_a^i, was increased from 1% to 8%. The recovery strain for each cycle, ε_R^i, is the difference between the applied strain and the residual strain (ε_a^i-$\varepsilon^i{}_r$). It is related to the relative strain increment from the previous cycle, $\Delta\varepsilon_a^i = (\varepsilon_a^i - \varepsilon_r^{i-1})$.

The relationship between recovery strain, ε_R^i, and the relative strain increment, $\Delta\varepsilon_a^i$, of the foams with different long-time and cyclic heat treatments, or various oligocrystallinity, is shown in Fig. 10(a). The recovery strain increases with increasing relative strain. The maximum recovery strain, ε_R^{MAX}, for each sample is obtained at the final cycle and is listed in Table 1. The dependence of the maximum recovery strain on oligocrystallinity is shown in Fig. 10(b). It can be seen that the maximum recovery strain has a strong dependence on oligocrystallinity, increasing linearly with *d/N* with a high linear fitting R-square of 0.993. The Cu-Al-Mn SMF specimen after CHT for 16 cycles ($d/N = 7.88$) exhibits a large recovery strain of 5.53%. This recovery strain contains both the pseudoelastic recovery strain of the shape memory alloy matrix

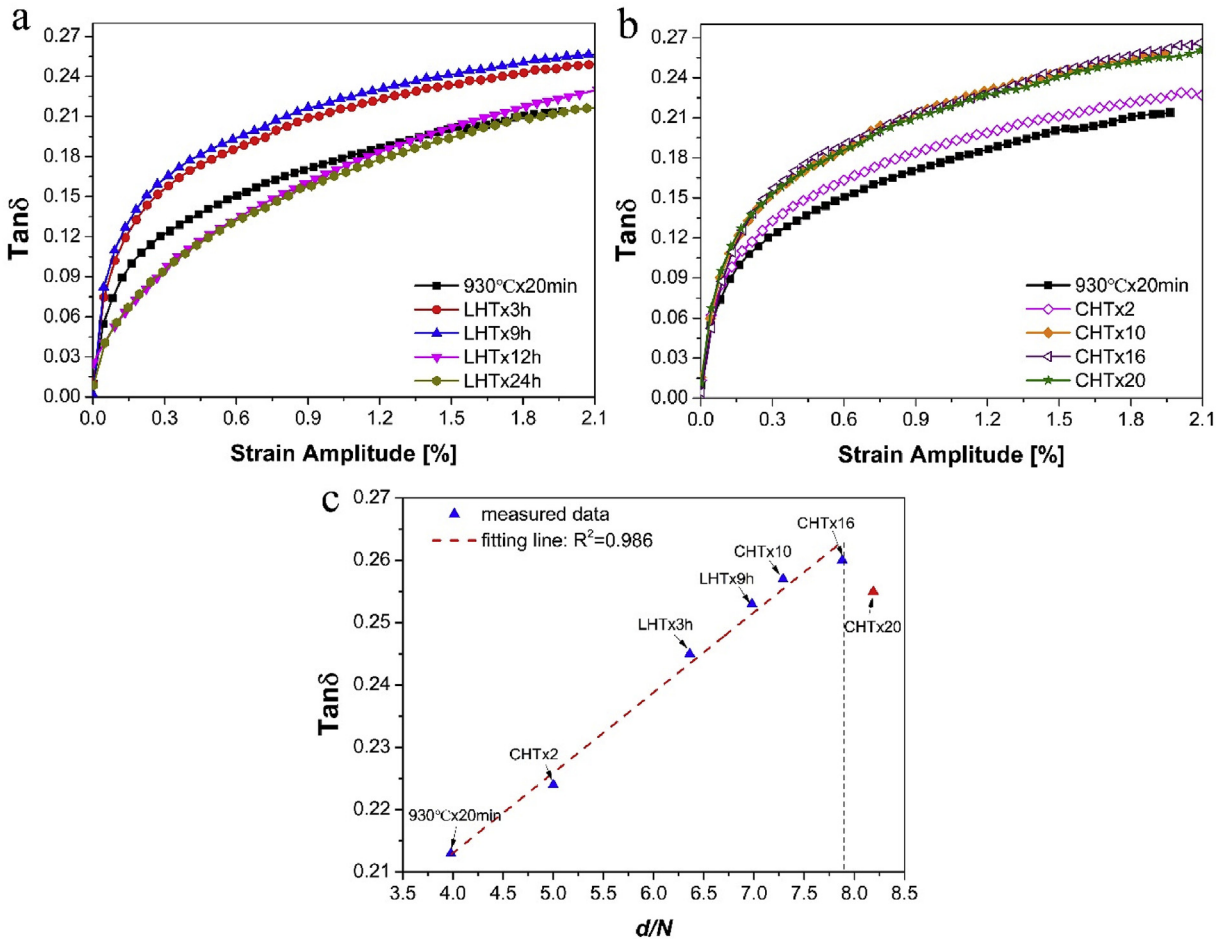

Fig. 8. Internal friction (tanδ) - (strain amplitude) curves of the Cu-Al-Mn SMFs subjected to (a) long-time and (b) cyclic heat treatments; (c) Dependence of high-amplitude martensite damping on oligocrystallinity (*d/N*) of the Cu-Al-Mn SMFs.

and the elastic recovery strain from the bucking and bending of the pore struts [29]. The increased recovery strain, however, should be attributed to the increased oligocrystallinity, which favors the stress-induced martensite transformation by relaxation of grain constraints. The relaxation of grain constraints is achieved mainly by reducing the grain boundary area and eliminating triple junctions, through enlarging grains by heat treatment. In foams with a higher *d/N*, there is a more unconstrained area where the stress-induced martensite transformation can progress more smoothly and more martensite plates can recover after unloading, leading to higher recovery strains.

The maximum recovery strain obtained in the Cu-Al-Mn oSMFs, although impressive, is still lower than those obtained in dense Cu-Al-Mn oSMAs. The pseudoelastic strain in dense Cu-Al-Mn oSMA wires and sheets reached 7%–8% when the oligocystallinity of wires (*d/D*) and sheets (*d/t*) grew to the critical values of 6.0 [24] and 15.4 [9], respectively. Obviously, the critical *d/t* of sheets is considerably greater than the critical *d/D* of wires, most likely because of the more complicatedly constrained grains in sheets than in wires. The constraint situation of grains in foam materials is even more complex. Firstly, stress concentration exists in the porous structure with a high porosity of ~70% when it is loaded and may lead to martensite stabilization while unloading and thus increase residual strain. Secondly, the intrinsic high grain anisotropy in SMFs may cause transformation incompatibility and increase slip defects between the grains [17], which is reflected by the different grain contrasts shown in Figs. 3 and 7. Thirdly, the intrinsic three-dimensional grain constraints of the foam structure may limit the optimum recovery property of oSMFs, although significant improvement of the recovery strain has been achieved by improving the ratio of the unconstrained area inside grains and near the free surface to the constrained area near boundaries and triple junctions. In view of the above, we expect that a higher critical *d/N* value is required to obtain an optimum performance of the Cu-Al-Mn oSMFs.

It should also be noticed that the strength of the shape memory foams changes little with oligocrystallinity. As shown in Fig. 8, the critical stress values (σ_M) for the stress-induced martensitic transformation of all the SMFs are in a narrow range of 19–23 MPa. The behavior resembles the situation observed in Cu-Al-Mn sheets [9]. It is reported that σ_M of the oSMA sheets [9] is sensitive to the three-dimensional grain constraints, with σ_M decreasing from ~350 MPa to ~100 MPa as *d/t* increases to the critical value of $d/t = 2$. However, after the grains become a full columnar structure and free from three-dimensional grain constraints, σ_M of the sheet remains unchanged as *d/t* increases further. It is therefore reasonable that σ_M of our Cu-Al-Mn oSMFs with intrinsic three-dimensional grain constraints behaves insensitively to *d/N*.

4. Conclusions

1) The average grain size in the Cu-Al-Mn SMFs after cyclic heat treatment is greater than after long-time heat treatment, reaching 3.44 mm after CHT for 20 cycles (10.5 h),

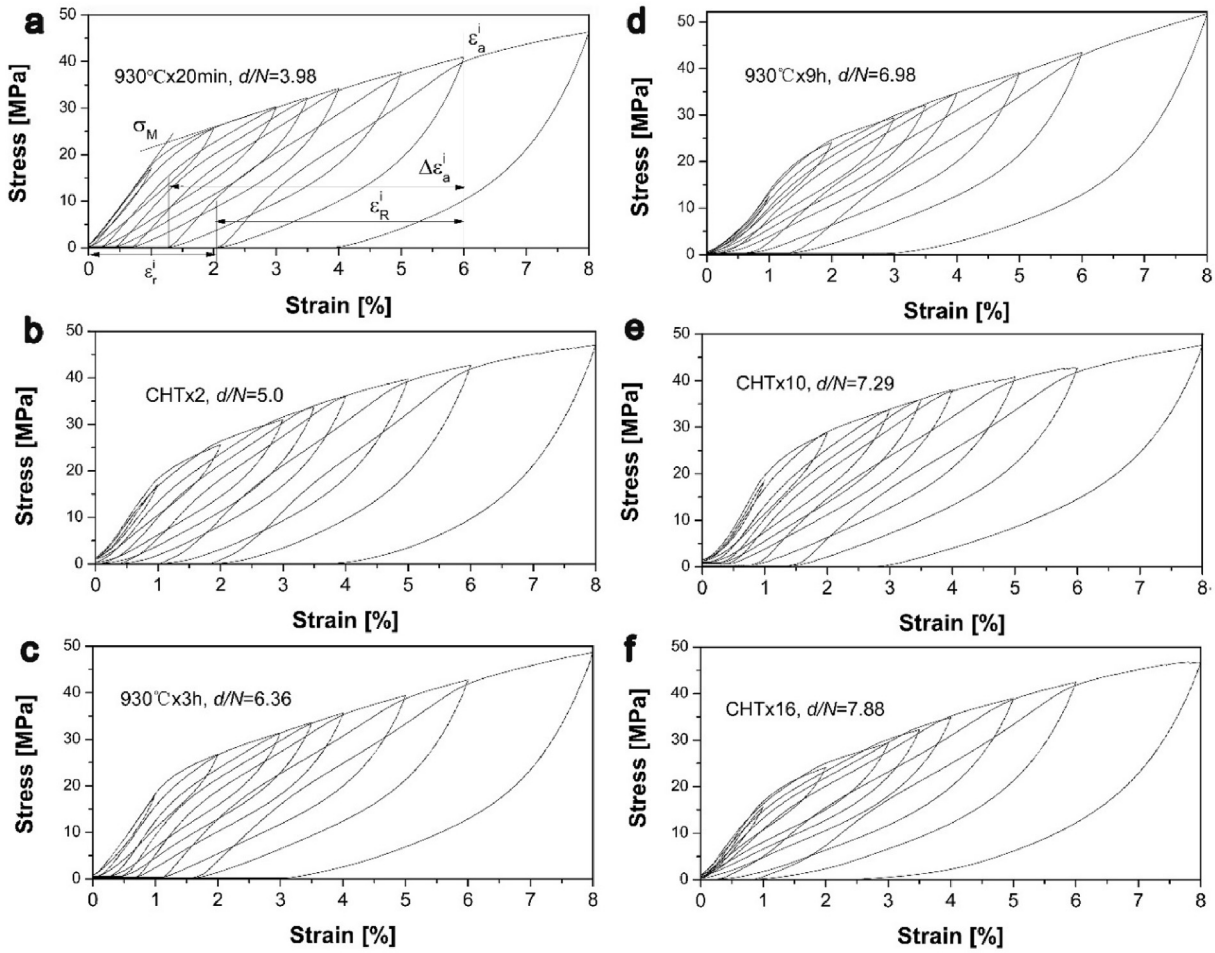

Fig. 9. Stress-strain curves of the Cu-Al-Mn SMFs after different long-time and cyclic heat treatments and with various oligocrystallinity values.

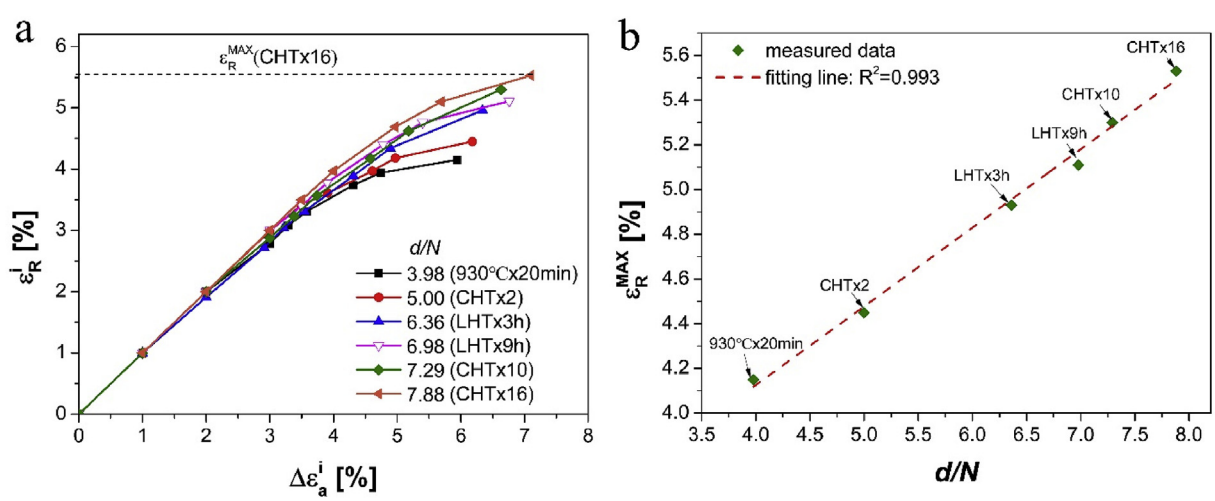

Fig. 10. (a) Relationship between recovery strain (ε_R^i) and relative strain ($\Delta\varepsilon_a^i$); (b) Dependence of maximum recovery strain (ε_R^{MAX}) on oligocrystallinity (d/N) of the Cu-Al-Mn SMFs.

corresponding to an oligocrystallinity (d/N) of 8.19. However, the average grain size and oligocrystallinity are much lower than those of Cu-Al-Mn oSMA sheets obtained under the similar conditions, due to the restriction effect of the complex strut architecture on grain growth. Holding time no more than 10.5 h is recommended to avoid property deterioration caused by loss of alloying elements.

2) The peak damping of the Cu-Al-Mn SMFs increases with oligocrystallinity because a higher oligocrystallinity favors the mobility of habit planes and martensite accommodation during martensitic transformation. The low-amplitude martensite

damping first increases and then decreases with increasing oligocrystallinity. The decreasing martensite damping in the latter is because the lower constraints of higher oligocrystallinity allow the martensite plate growing wider, which results in less martensite interface density. In contrast, the high-amplitude martensite damping increases linearly with oligocrystallinity, indicating that the mobility of martensite plates at high displacement is largely favored by lower grain constraints and can counterbalance the negative effect of wider martensite plates on damping.

3) The maximum recovery strain of the Cu-Al-Mn SMFs increases linearly with oligocrystallinity, reaching a high value of 5.53% after CHT for 16 cycles ($d/N = 7.88$). The impressive improvement is a consequence of the reduced triple junctions and grain boundary area due to grain enlargement, which lowers the grain constraints for stress-induced martensitic transformation and the recovery process. The strength of the SMFs does not change much with increasing oligocrystallinity.

Acknowledgment

The authors acknowledge the financial support from the Natural Science Foundation of Guangdong Province (2016A030311012), the National Natural Science Foundation of China (51571090) and the China Scholarship Council (201706150040).

References

[1] S. Nermat-Nasser, Y. Su, W.G. Guo, Experimental characterization and micromechanical modeling of superelastic response of a porous NiTi shape-memory alloy, J. Mech. Phys. Solid. 53 (2005) 2320–2346.
[2] J. Banhart, Manufacture, characterisation and application of cellular metals and metal foams, Prog. Mater. Sci. 46 (2001) 559–632.
[3] L. Delaey, R.V. Krishnan, H. Tas, et al., Thermoelasticity, pseudoelasticity and the memory effects associated with martensitic transformations, J. Mater. Sci. 9 (1974) 1521–1535.
[4] B. Yuan, P. Zheng, Y. Gao, et al., Effect of directional solidification and porosity upon the superelasticity of Cu–Al–Ni shape-memory alloys, Mater. Des. 80 (2015) 28–35.
[5] H. Li, B. Yuan, Y. Gao, Achieving high oligocrystalline degree via strut architecture tailoring to increase the damping and mechanical properties of spherical porous CuAlMn SMAs, J. Alloys Compd. 767 (2018) 690–702.
[6] W. Huang, On the selection of shape memory alloys for actuators, Mater. Des. 23 (2002) 11–19.
[7] S.M. Ueland, Y. Chen, C.A. Schuh, Oligocrystalline shape memory alloys, Adv. Funct. Mater. 22 (2012) 2094–2099.
[8] Y. Chen, X. Zhang, D.C. Dunand, et al., Shape memory and superelasticity in polycrystalline Cu–Al–Ni microwires, Appl. Phys. Lett. 95 (2009), 171906.
[9] Y. Sutou, T. Omori, R. Kainuma, et al., Grain size dependence of pseudoelasticity in polycrystalline Cu–Al–Mn-based shape memory sheets, Acta Mater. 61 (2013) 3842–3850.
[10] Y. Araki, T. Endo, T. Omori, et al., Potential of superelastic Cu–Al–Mn alloy bars for seismic applications, Earthq. Eng. Struct. Dynam. 40 (2011) 107–115.
[11] T. Kusama, T. Omori, T. Saito, et al., Two- and three-dimensional grain growth in the Cu-Al-Mn shape memory alloy, Mater. Trans. 54 (2013) 2044–2048.
[12] L.J. Gibson, Mechanical behavior of metallic foams, Annu. Rev. Mater. Sci. 30 (2000) 191–227.
[13] D.J. Thewsey, Y.Y. Zhao, Thermal conductivity of porous copper manufactured by the lost carbonate sintering process, Phys. Status Solidi 205 (2008) 1126–1131.
[14] F. Han, G. Seiffert, Y. Zhao, et al., Acoustic absorption behaviour of an open-celled aluminium foam, J. Phys. D Appl. Phys. 36 (2003) 294–302.
[15] M.W.D. Van der Burg, V. Shulmeister, E. Van der Geissen, et al., On the linear elastic properties of regular and random open-cell foam models, J. Cell. Plast. 33 (1997) 31–54.
[16] S. Gong, Z. Li, G.Y. Xu, N. Liu, Y.Y. Zhao, Fabrication, microstructure and property of cellular CuAlMn shape memory alloys produced by sintering–evaporation process, J. Alloys Compd. 509 (2011) 2924–2928.
[17] S.M. Ueland, C.A. Schuh, Grain boundary and triple junction constraints during martensitic transformation in shape memory alloys, J. Appl. Phys. 114 (2013), 053503.
[18] S. Miyazaki, K. Otsuka, H. Sakamoto, et al., The fracture of Cu–Al–Ni shape memory alloy, Trans. Jpn. Inst. Met. 22 (1981) 244–252.
[19] H. Li, B. Yuan, Y. Gao, Processing of CuAlMn shape memory foams with open spherical pores by silica-gel beads infiltration method, Metall. Mater. Trans. B 47 (2016) 3168–3177.
[20] P.A. Beck, P.R. Sperry, Strain induced grain boundary migration in high purity aluminum, J. Appl. Phys. 21 (1950) 150–152.
[21] T. Omori, T. Kusama, S. Kawata, et al., Abnormal grain growth induced by cyclic heat treatment, Science 341 (2013) 1500–1502.
[22] R. Kainuma, S. Takahashi, K. Ishida, Thermoelastic martensite and shape memory effect in ductile Cu-Al-Mn alloys, Metall. Mater. Trans. A 27 (1996) 2187–2195.
[23] Y. Sutou, T. Omori, R. Kainuma, et al., Ductile CuAlMn based shape memory alloys: general properties and applications, Met. Sci. 24 (2008) 896–901.
[24] Y. Sutou, T. Omori, K. Yamauchi, et al., Effect of grain size and texture on pseudoelasticity in Cu–Al–Mn-based shape memory wire, Acta Mater. 53 (2005) 4121–4133.
[25] E. Underwoood, Quantitative Stereology, Addison-Wesley, Massachusetts, USA, 1970, pp. 79–108.
[26] Y. Zheng, C. Li, F. Wan, Y. Long, Cu-Al-Mn alloy with shape memory effect at low temperature, J. Alloys Compd. 441 (2007) 317–322.
[27] J. San Juan, M.L. Nó, Damping behavior during martensitic transformation in shape memory alloys, J. Alloys Compd. 355 (2003) 65–71.
[28] J.N. Wei, H.F. Cheng, C.L. Gong, et al., Effects of macroscopic pores on the damping behavior of foamed commercially pure aluminum, Metall. Mater. Trans. A 33 (2002) 3565–3568.
[29] L.J. Gibson, Mechanical behavior of metallic foams, Annu. Rev. Mater. Sci. 30 (2000) 191–227.